

# Capacity Allocation and Optimal Control of Inverter Air Conditioners Considering Area Control Error in Multi-area Power Systems

Hongxun Hui, *Student Member, IEEE*, Yi Ding, *Member, IEEE*, Zhenzhi Lin, *Member, IEEE*, Pierluigi Siano, *Senior Member, IEEE*, and Yonghua Song, *Fellow, IEEE*

**Abstract**—Air conditioners (ACs) have been widely considered as one of the most important reserve resources for power systems. However, few attentions have been given to inverter ACs (IACs), which account for a larger share nowadays and show more suitable characteristics than regular ACs to provide reserve. Moreover, interconnected power systems are becoming increasingly large and complex, which puts forward higher request on the reserve resources for the system's reliability and safety. Dealing with the above challenges, this paper proposes a novel frequency regulation model of multi-area power systems considering large-scale IACs providing regulation service. In order to decrease the impact on customers' comfort, the action number constraint (ANC) and action time constraint (ATC) of IACs can be set by each customer. On this basis, the scheduling model of IACs considering ANC and ATC is proposed in multiple time scales, in which the total regulation capacity of IACs can be allocated among days in the month and areas in the multi-area power systems. Besides, the control parameters of IACs can also be optimized by the proposed optimization model for minimizing the area control error of the power system. The effectiveness of the model and method are verified in the numerical studies.

**Index Terms**—Inverter air conditioners, regulation service, area control error, multi-area power systems.

## NOMENCLATURE

### A. Acronyms

|     |                              |
|-----|------------------------------|
| AC  | Air conditioner              |
| ACE | Area control error           |
| AGC | Automatic generation control |
| ANC | Action number constraint     |
| ATC | Action time constraint       |
| DSR | Demand side resource         |

Manuscript received November 4, 2018; revised April 22, 2019, and accepted June 16, 2019. This work was supported in part by the National Key Research and Development Program of China under Grant 2016YFB0901100 and the National Science Foundation of China under Grant 51577167. Paper no. TPWRS-01678-2018. (*Corresponding author: Yi Ding*.)

H. Hui, Y. Ding, and Z. Lin are with the College of Electrical Engineering, Zhejiang University, Hangzhou 310027, China (e-mail: huihongxun@zju.edu.cn; yiding@zju.edu.cn; linzhenzhi@zju.edu.cn).

P. Siano is with the Department of Industrial Engineering, University of Salerno, Salerno 84084, Italy (e-mail: psiano@unisa.it).

Y. Song is with the State Key Laboratory of Internet of Things for Smart City and the Department of Electrical and Computer Engineering, University of Macau, Macau 999078, China, and also with the College of Electrical Engineering, Zhejiang University, Hangzhou 310027, China (e-mail: yhsong@umac.mo).

Color versions of one or more of the figures in this paper are available online at <http://ieeexplore.ieee.org>.

|                                    |   |
|------------------------------------|---|
| IAC                                | Inverter air conditioner  |
| PI                                 | Proportional-integral   |
| <b>B. Variables and parameters</b> |   |
| $k$                                | Index of an individual IAC  |
| $i, j$                             | Index of the area in multi-area power systems   |
| $N_A$                              | Total number of areas   |
| $N_i$                              | Total number of IACs in area- $i$   |
| $c_A$                              | Heat capacity of the air  |
| $\rho_A$                           | Heat density of the air   |
| $V$                                | Room volume   |
| $A_S$                              | Surface area of the room  |
| $\xi$                              | Air exchange times  |
| $T_A$                              | Indoor temperature  |
| $T_O$                              | Ambient temperature   |
| $T_{set}$                          | Set temperature of the IAC  |
| $T_{dev}$                          | Deviation between $T_A$ and $T_{set}$   |
| $Q_{gain}$                         | Total heat gains of the room  |
| $Q_{IAC}$                          | Cooling capacity of the IAC   |
| $Q_{dis}$                          | Heat radiation in the room  |
| $U_{HT}$                           | Heat transfer coefficient   |
| $\kappa_p, \mu_p$                  | Power coefficients of the IAC   |
| $\kappa_Q, \mu_Q$                  | Heat coefficients of the IAC  |
| $f_c$                              | Operating frequency of the compressor   |
| $\Delta f_i$                       | System frequency deviation in area- $i$   |
| $\theta, \eta$                     | PI controller coefficients of the compressor  |
| $\beta$                            | Integral controller coefficient of the ACE  |
| $\delta_i, \gamma_i$               | Proportional controller coefficients of the ACE   |
| $S_{IAC,k}$                        | Controllable state of IAC- $k$  |
| $\Delta P_{Tie,i}$                 | Tie line power deviation in area- $i$   |
| $\Delta P_{IAC,k}$                 | Regulation capacity provided by IAC- $k$  |
| $\Delta P_{IAC,i}$                 | Total available regulation capacities provided by IACs in area- $i$                         |
| $\Delta P_{L,i}$                   | Disturbance power   |
| $F_{HP,i}$                         | Power fraction of the reheat turbine in area- $i$   |
| $R_{G,i}$                          | Governor speed regulation parameter   |
| $B_{G,i}$                          | Frequency bias parameter  |
| $K_{G,i}$                          | Integral gain of the generator  |
| $T_{p,i}$                          | Inertia time constant of the area- $i$  |
| $K_{p,i}$                          | Frequency damping factor of the area- $i$   |
| $N_{IAC}^{\max}$                   | Action number of IACs   |
| $P_{SHT}$                          | Shortage index of the regulation capacity   |
| $N_S$                              | Number of the disturbance scenarios   |
| $T_{g,i}, T_{t,i}, T_{r,i}$        | Time constants of the speed governor, the steam turbine, and the reheat module in area- $i$ |

## I. INTRODUCTION

THE increasing high temperature events in summer lead to the growing power consumption of air conditioners (ACs), for example, whose loads fetched up to 52% of the total loads in Beijing, China on July 12, 2017 [1]. The huge power consumption of ACs causes more events of electricity shortages, which will then give rise to the insufficient reserve resources for maintaining the system balance between supply and demand [2]. For instance, the blackout in Taiwan on August 15th, 2017 was fundamentally caused by the huge power consumption of ACs and the shortage of the regulation resources [3], [4]. Therefore, sufficient reserve capacity is important for the stability and security of the power system. Traditionally, the regulation services are provided by conventional generating units, such as the thermal power units and hydro power ones [5]. However, it may be uneconomical for the power system to increase the reserve capacity by building more conventional power plants [6]. The progressed information and communication technologies have also provided another alternative from demand-side [7]. It has been proved that demand side resources (DSRs) can provide the same regulation service as generators by adjusting the power consumption [8]. The DSRs can decrease, increase or transfer loads when the disturbance power or generator failures occur [9], [10].

Among the common household appliances (e.g., ACs, lights, washing machines, microwaves) [11], [12], ACs have been widely considered as one of the most important DSRs [13], [14]. Because the ACs have huge potential to be dispatched for providing reserve [1], and can be controlled to change the power consumption without significant influences on the customers' comfort [2]. For example, the interactive controller and the temperature-priority-list controller are used in [11] and [15], respectively, to dispatch ACs to provide balancing service for assisting power system operation, while at the same time guaranteeing the desired indoor temperatures of customers. The ACs can be divided into two categories, the regular fixed frequency ACs and inverter ACs (IACs). The compressors of the regular ACs can only operate in two modes, i.e., *on* or *off* mode, while the compressors of the IACs can be adjusted continuously [16]. Therefore, the IACs are more suitable to be controlled as DSRs to provide operating reserve compared with regular ACs. Besides, the market share of IACs is growing steadily, for instance, which has outnumbered regular ACs in China [17]. Therefore, it is significant to study IACs for providing regulation services.

Moreover, the interconnected power systems are becoming larger and more complex, which proposes higher request on the system reserve capacity for the quality and stability of the power system [18]. It will result in more serious consequences when the disturbance power occurs in the multi-area power systems, including system frequency deviations and tie line power deviations. Dealing with this problem, the area control error (ACE) is becoming one of the most important parameters in the multi-area power systems, which considers both the system frequency control and tie line power deviation control [19], [20]. On this basis, the generators and DSRs in the

multi-area power systems can not only provide regulation services for its area, but also for other areas [21].

However, the existing researches on the frequency regulation in the multi-area power systems mainly focus on the optimization of generators' control parameters [18], [19] or DSRs' control parameters [20], [21], whereas the regulation capacity allocation method provided by DSRs in the multi-area power systems has rarely been studied. The authors in [22] develop the electrical model of IACs, while the balancing effect of IACs on the power system is not considered. The state-queueing control method of DSRs for providing regulation services is proposed in [23], while the DSRs are assumed to be controlled only in *on/off* states and cannot be adjusted continuously as IACs. The temperature adjustment control method of ACs is proposed in [2] to provide reserve resources for the power system, while it only analyzes the effectiveness in the minute-time scale and does not carry out the studies in the second-time scale for the power system's frequency control. The aggregation of IACs in [24] are equivalent to a reheat steam generator and can be controlled to provide frequency regulation service for the power system, while it only studies the control method in a single-area power system. The hybrid dynamic demand control strategy of ACs is proposed in [25] to deal with the increasing fluctuations brought by renewable energies, whereas it only optimizes the control parameters and does not consider the regulation capacity allocation in the multi-area power systems. Consequently, the research on IACs for providing regulation service in the multi-area power system is not sufficient.

To deal with the above problems, this paper develops a novel frequency regulation model of multi-area power systems with large-scale IACs providing regulation services. In order to decrease the impact on customers' comfort, the action number constraint (ANC) and action time constraint (ATC) of IACs can be set by each customer before the beginning of the month. On this basis, the scheduling model of IACs considering ANC and ATC is proposed in multiple time scales, in which the total regulation capacity of IACs can be allocated among days in the month and areas in the multi-area power systems. Besides, the control parameters of IACs in each area can also be optimized combined with the allocated capacities by the proposed optimization model for minimizing the ACE. The main contributions of this paper can be summarized as follows:

(1) The frequency regulation model of multi-area power systems considering large-scale IACs providing frequency regulation service is proposed for the first time in the existing researches. On this basis, the control strategy considering ACE of the multi-area power systems and the regulation capacity evaluation method of IACs are also proposed.

(2) A novel scheduling model of IACs in multiple time scales (month, day and real-time) is developed to allocate the regulation capacities among days and areas in the multi-area power systems, and in which the control parameters of IACs can also be optimized combined with the allocated regulation capacities. Besides, the customers' comfort can also be guaranteed by considering the action number constraints and action time constraints of the IACs.

(3) The effectiveness of the model and method are verified in the numerical studies, which is based on the actual environment parameters and IACs' parameters. The comparison analysis between IACs and regular ACs is also carried out to verify the advantages of IACs for providing frequency regulation service.

The remaining of this paper is organized as follows. Section II proposes the modeling method and control strategy of IACs. Then the frequency regulation model of the multi-area power systems considering the regulation services provided by large-scale IACs are developed in Section III. The scheduling model and optimization method of IACs are proposed in Section IV. Numerical studies are carried out in Section V, and finally Section VI concludes this paper.

## II. MODELLING AND CONTROL STRATEGY OF IACs

### A. Thermal and Electric Model of IACs

The operating power of the IAC is closely related to the thermal characteristics of the room. Therefore, it is essential to build the thermal model of the room for studying the operating characteristic of the IAC. The thermal model of the room can be expressed as [2]:

$$c_A \rho_A V \frac{dT_A(t)}{dt} = Q_{gain}(t) - Q_{IAC}(t) \quad (1)$$

where  $c_A$  and  $\rho_A$  are the heat capacity and density of the air, respectively.  $V$  and  $T_A$  are the room volume and the indoor temperature, respectively.  $Q_{gain}$  is the heat gain of the room.  $Q_{IAC}$  is the cooling capacity of the IAC.

The heat gain  $Q_{gain}$  comes from the heat transfer between the indoor and outdoor air, which can be described as [24]:

$$Q_{gain}(t) = (U_{HT} A_s + c_A \rho_A V \xi)(T_o(t) - T_A(t)) + Q_{dis}(t) \quad (2)$$

where  $U_{HT}$  is the heat transfer coefficient.  $A_s$  is the surface area of the room.  $\xi$  is the air exchange times between the indoor and outdoor air as a result of the open doors and windows.  $T_o$  is the ambient temperature.  $Q_{dis}$  is the heat radiation from lights, people and other disturbance factors.

The cooling capacity of the IAC is related to the operating frequency of the compressor, which can be expressed as:

$$Q_{IAC}(t) = \kappa_Q f_c(t) + \mu_Q \quad (3)$$

where  $\kappa_Q$  and  $\mu_Q$  are the constant coefficients of the IAC.  $f_c$  is the operating frequency of the compressor, which can be adjusted in a certain range, as shown below.

$$f_c^{\min} \leq f_c(t) \leq f_c^{\max} \quad (4)$$

Similarly, the power consumption of the IAC is also related to the operating frequency of the compressor and can be expressed as:

$$P_{IAC}(t) = \kappa_p f_c(t) + \mu_p \quad (5)$$

where  $\kappa_p$  and  $\mu_p$  are the constant coefficients of the IAC, respectively.

### B. Control Strategy of IACs for Providing Regulation Service

As for the normal IAC- $k$ , which does not provide regulation service for the power system, the control objective is to maintain the indoor temperature equal to the set temperature. The control target of the compressor frequency can be realized by the proportional integral (PI) controller [24]:

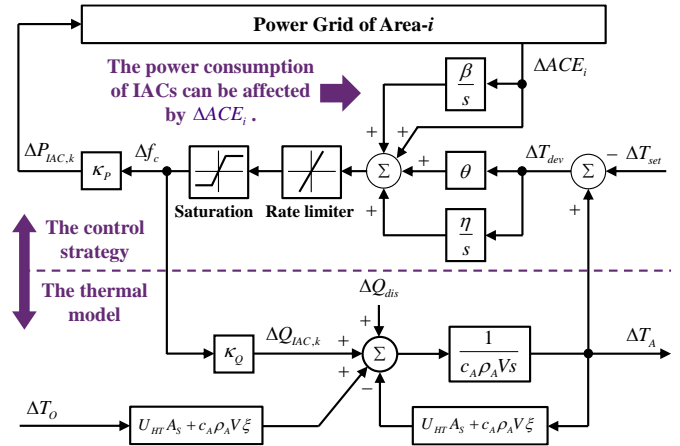


Fig. 1. The transfer function model of the IAC for providing regulation service.

$$\Delta f_{c,k}(t) = \theta \cdot T_{dev,k}(t) + \eta \cdot \int T_{dev,k}(t) dt \quad (6)$$

$$T_{dev,k}(t) = T_{A,k}(t) - T_{set,k}(t) \quad (7)$$

where  $\theta$  and  $\eta$  are the constant coefficients of the controller.  $T_{dev,k}$  is the temperature deviation between the indoor temperature and the set temperature.

However, if the IAC- $k$  could provide regulation service in the multi-area power systems, the operating frequency of the compressor should be impacted not only by the temperature deviation  $T_{dev,k}$ , but also by the power system frequency deviation or the tie line power deviation. Therefore, the control strategy can be extended from the Eq. (6), which can be described as:

$$\Delta f_{c,k}(t) = \theta \cdot T_{dev,k}(t) + \eta \cdot \int T_{dev,k}(t) dt + \Delta ACE_i(t) + \beta \cdot \int \Delta ACE_i(t) dt \quad (k \in N_i) \quad (8)$$

where  $\Delta ACE_i(t)$  is the area control error (ACE) in area- $i$ .  $\beta$  is the integral controller coefficient of the ACE.  $N_i$  is the total number of IACs in area- $i$ . The regulation capacity provided by the IAC- $k$  can be deduced from the Eq. (5) and Eq. (8), and expressed as:

$$\Delta P_{IAC,k}(t) = \kappa_p \Delta f_{c,k}(t) \quad (k \in N_i) \quad (9)$$

Besides, the IACs in area- $i$  can share the responsibility of the ACE. Therefore, the total available regulation capacities provided by IACs in area- $i$  can be calculated by:

$$\Delta P_{IAC,i}(t) = \sum_{k \in N_i} \Delta P_{IAC,k}(t) \cdot S_{IAC,k}(t) \quad (10)$$

where  $S_{IAC,k}$  is the controllable state of IAC- $k$ , which is equal to 1 if the IAC is in the *on*-state and controllable, while  $S_{IAC,k}$  will be 0 when the IAC is uncontrollable or in the *off*-state.

ACE is an important parameter in the multi-area power systems and used as the key index for the control of the system frequency and the transfer power among areas [18]. The ACE is calculated by the power system frequency deviation and the tie line power deviation, which can be expressed as:

$$\Delta ACE_i(t) = \delta_i \Delta f_i(t) + \gamma_i \Delta P_{tie,i}(t) \quad (11)$$

where  $\Delta f_i$  and  $\Delta P_{tie,i}$  are the system frequency deviations and the tie line power deviations in area- $i$ , respectively.  $\delta_i$  and  $\gamma_i$  are the proportional controller coefficients of the IACs in area- $i$ , respectively.

Based on the above thermal and electric model of the IAC and the control strategy of the compressor, the transfer function model of the IAC can be developed, as shown in Fig. 1. It can be seen that the operating power of the IAC is affected mainly by four factors, the ambient temperature deviation  $\Delta T_o$ , the heat radiation deviation  $\Delta Q_{dis}$ , the set temperature  $\Delta T_{set}$  and  $\Delta ACE_i$ , respectively. Generally, the duration of the IAC control for providing regulation reserve is short, e.g., 30 seconds for the primary frequency control and 15 minutes for the secondary frequency control [24]. Therefore, as for the IAC operating in the stable state, the ambient temperature, the set temperature and the heat radiation can be regard as invariable during the short period of the control process, and thus the regulation power of the IAC is mainly related to  $\Delta ACE_i$ . Moreover, the cooling capacity of the IAC will be impacted, when the IAC is controlled to provide regulation reserve. It comes with the indoor temperature deviations. In order to decrease the impact on customers, the indoor temperature should be constrained in an acceptable range, which can be described as:

$$\Delta T_A^{\min} \leq \Delta T_A \leq \Delta T_A^{\max} \quad (12)$$

where  $\Delta T_A^{\min}$  and  $\Delta T_A^{\max}$  are the minimum and maximum acceptable indoor temperature deviations, respectively.

### C. Regulation Capacity Evaluation of IACs

As for the IAC operating in the stable state, the indoor temperature  $T_A$  is controlled to be steady near the set temperature  $T_{set}$ . At that time, the cooling capacity of the IAC approximately equals to the heat gain of the room, which can be expressed as:

$$Q_{gain}(t) = Q_{IAC}(t) \quad (13)$$

Therefore, the operating frequency of the compressor can be derived and described as:

$$f_c(t) = \left[ (U_{HT} A_s + c_A \rho_A V \xi)(T_o(t) - T_{set}(t)) \right] / \kappa_Q + [Q_{dis}(t) - \mu_Q] / \kappa_Q \quad (14)$$

Then the operating power of the IAC in the stable state can be expressed as:

$$P_{IAC}(t) = \kappa_P \left[ (U_{HT} A_s + c_A \rho_A V \xi)(T_o(t) - T_{set}(t)) \right] / \kappa_Q + \kappa_P Q_{dis}(t) / \kappa_Q + (\kappa_Q \mu_p - \kappa_P \mu_Q) / \kappa_Q \quad (15)$$

Due to the adjustment ranges of the compressor's frequency, the operating power of the IAC can be adjusted in the below ranges.

$$\kappa_P f_c^{\min} + \mu_p \leq P_{IAC}(t) \leq \kappa_P f_c^{\max} + \mu_p \quad (16)$$

Therefore, maximum available capacities of the IAC for providing up and down regulation services can be calculated by the Equations (15)-(16), which can be expressed as  $\Delta P_{IAC}^{up,\max}$  and  $\Delta P_{IAC}^{down,\max}$ , respectively, as shown in Fig. 2.

Fig. 2 illustrates the operating frequency of the compressor and the operating power of the IAC in the stable state, which will change under different ambient temperatures and set temperatures. When the set temperature is fixed and equal to 24°C, as shown in Fig. 2(a),  $f_c$  and  $P_{IAC}$  will be larger with the increase of  $T_o$ , owing to the increasing flow of the outdoor hot air. By contrast, as shown in Fig. 2(b), the  $f_c$  and  $P_{IAC}$  will be

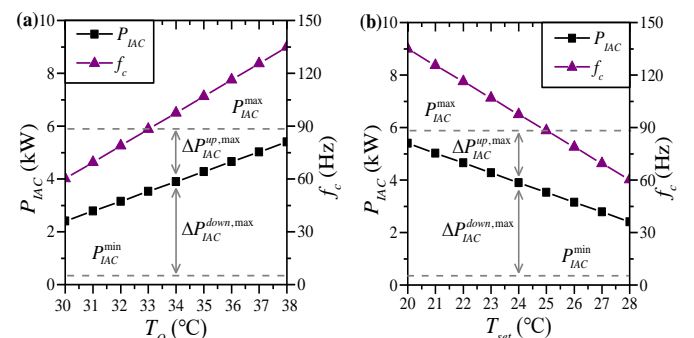


Fig. 2. The operating frequency of the compressor and the operating power of the IAC in the stable state. (a) The set temperature is 24°C. (b) The ambient temperature is 34°C.

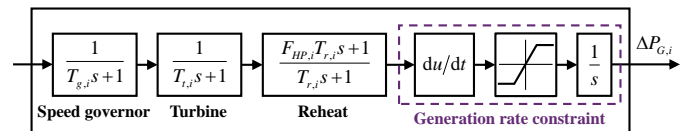


Fig. 3. The transfer function model of the reheat steam generator.

smaller with the increase of  $T_{set}$ , when the ambient temperature is identically equal to 34°C. Because the IAC can produce less cooling capacity to maintain a higher indoor temperature. Moreover, the dotted lines  $P_{IAC}^{\min}$  and  $P_{IAC}^{\max}$  in Fig. 2 are the minimum and maximum operating power of the IAC, respectively. Thus the maximum available capacities of the IAC for providing up and down regulation service can be described as the two arrows  $\Delta P_{IAC}^{up,\max}$  and  $\Delta P_{IAC}^{down,\max}$ , respectively.

Moreover, apart from the accurate calculation method as the Eq. (10), the total available regulation capacities of IACs can also be estimated by the average regulation power, which can be expressed as:

$$\Delta P_{IAC,i}(t) = \Delta P_{IAC,i}^{\text{avg}}(t) \cdot \sum_{k \in N_i} S_{IAC,k}(t) \quad (17)$$

where  $\Delta P_{IAC,i}^{\text{avg}}$  is the average regulation capacity of one IAC in area- $i$ , which can be calculated by the historical statistical data.

### III. FREQUENCY REGULATION MODELLING OF MULTI-AREA POWER SYSTEMS WITH CONTROLLABLE IACs

It is assumed that the IACs are installed with controllers and can be dispatched to adjust the power consumption to provide regulation service in the multi-area power systems. Then each area of the multi-area power system can be divided into three parts, the traditional generators, the controllable IACs and the other traditional loads, respectively. When the load fluctuates and the ACE occurs, both the power generation of the generators and the power consumption of the IACs will be regulated to assist the power system to rebalance.

As the studies have been carried out in [19], [20], [24], the generators in this paper are also assumed as reheat steam generators, whose transfer function model can be developed as shown in Fig. 3.  $T_{g,i}$ ,  $T_{t,i}$  and  $T_{r,i}$  are the time constants of the speed governor, the steam turbine, and the reheat module, respectively.  $F_{HP,i}$  is the power fraction of the reheat turbine. Moreover, the generation ramp rate constraint is considered in

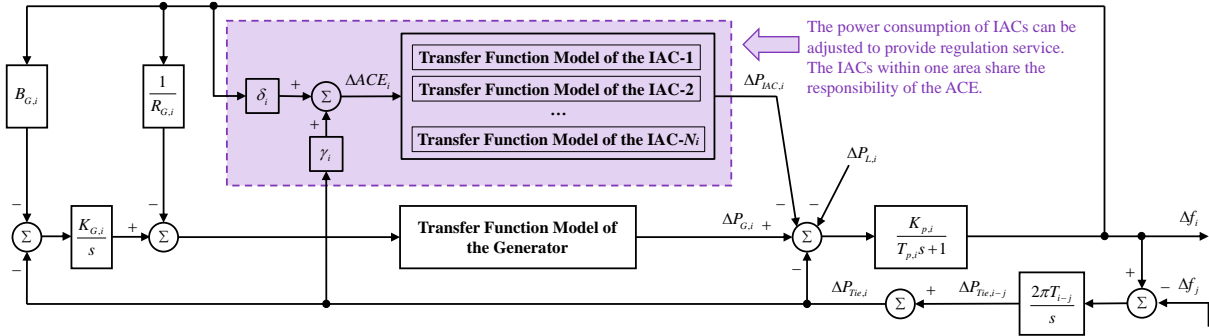


Fig. 4. The transfer function model of one area in the multi-area power systems.

this model, because it can also seriously impact the regulation effect of the system frequency control.

Based on the transfer function model of the IAC in Fig. 1 and the transfer function model of the reheat steam generator in Fig. 3, the multi-area power systems with controllable generators and IACs for providing regulation service can be developed. Fig. 4 shows the frequency regulation model of one area in the multi-area power systems [19], where  $R_{G,i}$ ,  $B_{G,i}$  and  $K_{G,i}$  are the governor speed regulation parameter, the frequency bias parameter, and the integral gain of the generator, respectively.  $T_{p,i}$  and  $K_{p,i}$  are the inertia time constant and frequency damping factor, respectively.  $\Delta P_{L,i}$  is the disturbance power. The tie line power deviation is defined as the variation of the transmission power with other areas of the power system, which can be calculated by:

$$\begin{aligned}\Delta P_{Tie,i}(t) &= \sum_{i,j \in N_A, j \neq i} \Delta P_{Tie,i-j}(t) \\ &= \sum_{i,j \in N_A, j \neq i} 2\pi T_{i-j} \int (\Delta f_i(t) - \Delta f_j(t)) dt\end{aligned}\quad (18)$$

where  $N_A$  is the total area number of the multi-area power systems.  $\Delta P_{Tie,i-j}$  and  $T_{i-j}$  are the tie line power deviation and the tie line time constant between area- $i$  and area- $j$ , respectively.

Moreover, the  $\Delta P_{Tie,i-j}$  is different for the two areas, area- $i$  and area- $j$ , because the rated system capacities of the two areas may be different. Therefore, the capacity conversion coefficient  $a_{ij}$  is proposed to deal with the different rated capacities between area- $i$  and area- $j$ , which can be expressed as:

$$a_{ij} = -P_{r,i}/P_{r,j}, (i, j \in N_A, i \neq j) \quad (19)$$

where  $P_{r,i}$  and  $P_{r,j}$  are the rated system capacities of area- $i$  and area- $j$ , respectively.

#### IV. SCHEDULING MODEL OF IACs CONSIDERING ACTION NUMBER AND ACTION TIME CONSTRAINTS

##### A. Action Number and Action Time Constraints of IACs

The scheduling model of IACs is developed on a monthly basis and the customers can decide to participate in the regulation service in each month. Meanwhile, in order to decrease the impact on the comfort, the action number constraints (ANC) and action time constraints (ATC) of the IACs in a month can be set by the customers before the beginning of the month. Therefore, the scheduling model of IACs should be developed in the premise of subjecting to ANC

and ATC. The ANC of IACs can be expressed as:

$$0 \leq ANC_{IAC,k}(t) \leq ANC_{IAC,k}^{\max} \quad (20)$$

where  $ANC_{IAC,k}(t)$  and  $ANC_{IAC,k}^{\max}$  are the actual and maximum action number of IAC- $k$ , respectively. The ATC of IACs can be expressed as two modes, i.e., 1 and 0.  $ATC_{IAC,k}(t)$  is equal to 1 on the allowable control days, while 0 on the other days.

As shown in Fig. 5, the scheduling model of IACs considering ANC and ATC can be divided into three steps. The first step is allocating the regulation capacity of IACs among days in the month, which should be carried out before the beginning of the month. Then the second step is allocating the regulation capacity of IACs among areas in the multi-area power systems in a day, which can be implemented before the beginning of the day. Moreover, the control parameters of IACs ( $\delta_i$  and  $\gamma_i$ ) and generators ( $B_{G,i}$  and  $K_{G,i}$ ) should also be calculated at this time. The third step is sequence scheduling and rolling modification of IACs in the real time. The implementation procedure is explained in the next subsections in detail.

##### B. Step 1: Regulation Capacity Allocation of IACs Among Days

The total regulation capacity of IACs in the month is limited considering the ANC and ATC. Therefore, the first step of the scheduling model is allocating the limited regulation capacity provided by IACs among days in the month. As for the large-scale IACs, the action number of IACs  $N_{IAC}^{\max}(t)$  can be regarded as the allocated regulation capacity, as the regulation capacity evaluation method in the Equation (17). Thus the regulation capacity allocation problem can be reducible to the action number allocation problem of IACs.

The main purpose of controlling IACs is to make up the shortage of the regulation capacity provided by generators, especially in high temperature days in summer, when the loads reach the peak value of the year and at the same time IACs become the main power consuming equipment [1]. Therefore, the allocation criterion of the IACs' action number on each day is based on the shortage of the regulation capacity, which can be expressed as:

$$N_{IAC}^{\max}(t) = \sum_{i \in N_A} \sum_{k \in N_i} ANC_{IAC,k}^{\max} \cdot P_{SHT}(t) / \sum_{i \in D} P_{SHT}(t) \quad (21)$$

$$P_{SHT}(t) = \max \left\{ 0, \sum_{i \in N_A} \Delta P_{R,i}^{\max}(t) - \sum_{i \in N_A} \Delta P_{G,i}^{\max}(t) \right\} \quad (22)$$

where  $N_{IAC}^{\max}(t)$  is the allocated action number of IACs on the

day- $t$ .  $P_{SHT}(t)$  is the shortage index of the regulation capacity provided by generators.  $\Delta P_{G,i}^{\max}(t)$  is the maximum regulation capacity of the generators in area- $i$ .  $\Delta P_{R,i}^{\max}(t)$  is the required regulation capacity for disturbance power, which can be obtained by load forecasting and the requirement on the reserve ratio in the power system.

However,  $N_{IAC}^{\max}(t)$  calculated by the above Equations (21)-(22) cannot be the final results of the action number, because  $N_{IAC}^{\max}(t)$  should also satisfy the second constraint (ATC), which can be expressed as:

$$N_{IAC}^{\max}(t) \leq \sum_{i \in N_A} \sum_{k \in N_i} ATC_{IAC,k}(t) \quad (23)$$

It means that if the inequality constraint (23) cannot be satisfied, the available IACs are insufficient on the day- $t$ . In this scenario, the exceeded  $N_{IAC}^{\max}(t)$  will be set to be equal to the maximum value, and the action number of IACs on other days will be calculated again by the Equations (21)-(22). The procedure of the scheduling model is shown in Fig. 5.

### C. Step 2: Regulation Capacity Allocation Among Areas and Control Parameter Optimization of IACs

The allocated action number of IACs calculated in the first step is the total available IACs in the multi-area power systems on day- $t$ , while the second step of the scheduling model is allocating  $N_{IAC}^{\max}(t)$  among the areas. Moreover, the control parameters of the IACs ( $\delta_i$  and  $\gamma_i$ ) and generators ( $B_{G,i}$  and  $K_{G,i}$ ) are also calculated at this time. The optimization model can be developed, in which the optimization parameters include  $N_{IAC,i}^{\max}(t)$ ,  $\delta_i$ ,  $\gamma_i$ ,  $B_{G,i}$  and  $K_{G,i}$ . The optimization objective is to minimize the ACE of the multi-area power systems, which can be expressed as [19], [20]:

$$\min \sum_{s \in N_s} \left( \sum_{i \in N_A} \int_0^{T_f} \Delta f_{s,i}(t)^2 dt + \sum_{i,j \in N_A, i \neq j} \int_0^{T_p} \Delta P_{tie,s,i-j}(t)^2 dt \right) \quad (24)$$

$$\text{s.t.} \quad \sum_{i \in N_A} N_{IAC,i}^{\max}(t) \leq N_{IAC}^{\max}(t) \quad (25)$$

$$0 \leq N_{IAC,i}^{\max}(t) \leq \sum_{k \in N_i} ATC_{IAC,k}(t), N_{IAC,i}^{\max}(t) \in \mathbb{Z} \quad (26)$$

$$\delta_i \geq 0, \delta_i \in \mathbb{R} \quad (27)$$

$$\gamma_i \geq 0, \gamma_i \in \mathbb{R} \quad (28)$$

$$B_{G,i} \geq 0, B_{G,i} \in \mathbb{R} \quad (29)$$

$$K_{G,i} \geq 0, K_{G,i} \in \mathbb{R} \quad (30)$$

where  $T_f$  and  $T_p$  are the duration time of the system frequency deviations and the tie line power deviations, respectively.  $N_{IAC,i}^{\max}(t)$  is the action number of IACs in area- $i$ .  $N_s$  is the number of the disturbance scenarios, which are usually caused by the load disturbances or the generating unit failures. The disturbance power may occur at any area of the multi-area power systems, and thus different scenarios are considered in the objective function instead of one scenario [19]. The optimization model can be solved by intelligence algorithms, such as the genetic algorithm [20] and particle swarm optimization algorithm [26], [27].

### D. Step 3: Sequence Scheduling and Rolling Modification of IACs in Real Time

The allocated number of IACs in each area can be obtained

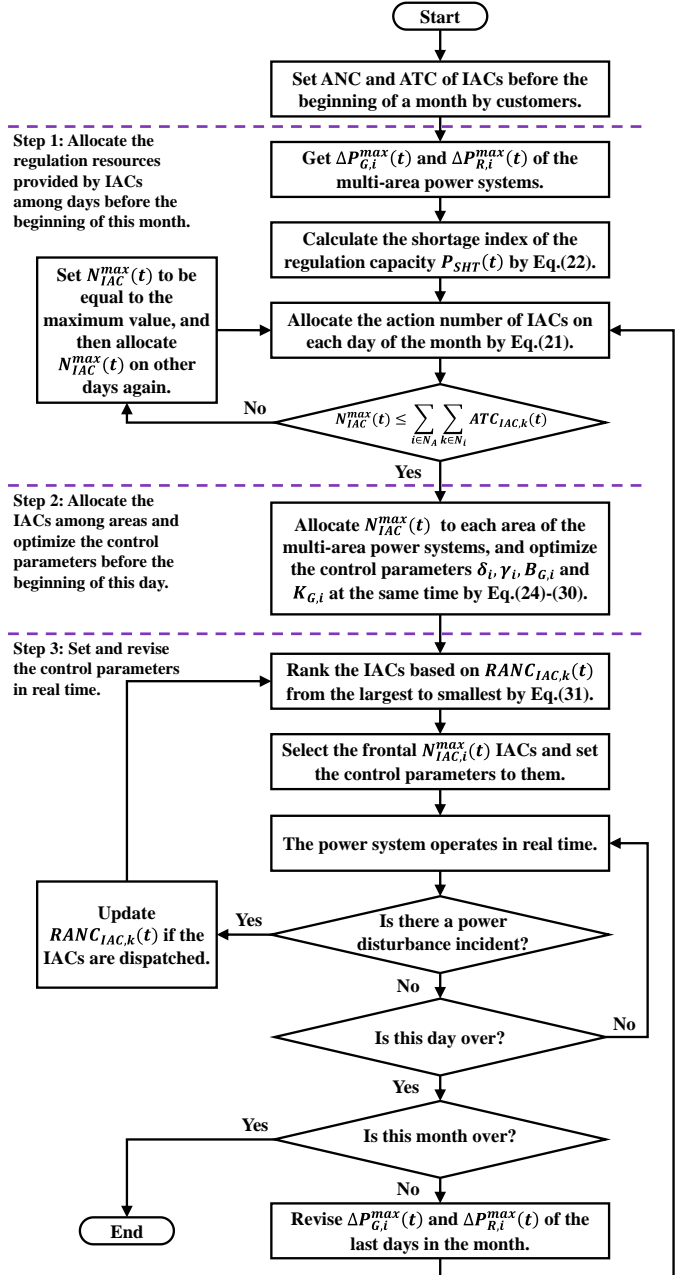


Fig. 5. The scheduling model of IACs considering action number constraints and action time constraints in different time scales (month, day, and real-time).

from the optimization model, which is generally less than the available IACs, as shown in the Equation (26). Thus the third step is to select  $N_{IAC,i}^{\max}(t)$  IACs in area- $i$  to be controlled as the parameters ( $\delta_i$ ,  $\gamma_i$ ,  $B_{G,i}$  and  $K_{G,i}$ ) in real time. The sequence scheduling method is proposed here based on the remaining action number of IACs, which can be expressed as:

$$RANC_{IAC,k}(t) = ANC_{IAC,k}^{\max} - ANC_{IAC,k}(t) \quad (31)$$

where  $RANC_{IAC,k}(t)$  is the remaining action number of the IAC- $k$  in this month. Then the IACs in area- $i$  can be ranked from the largest to the smallest based on the value of  $RANC_{IAC,k}(t)$ . The frontal  $N_{IAC,i}^{\max}(t)$  IACs will be selected and set as the control parameters. In this manner, the IACs can be dispatched in view of customers' desire and the impact on customers' satisfaction can also be reduced. During the

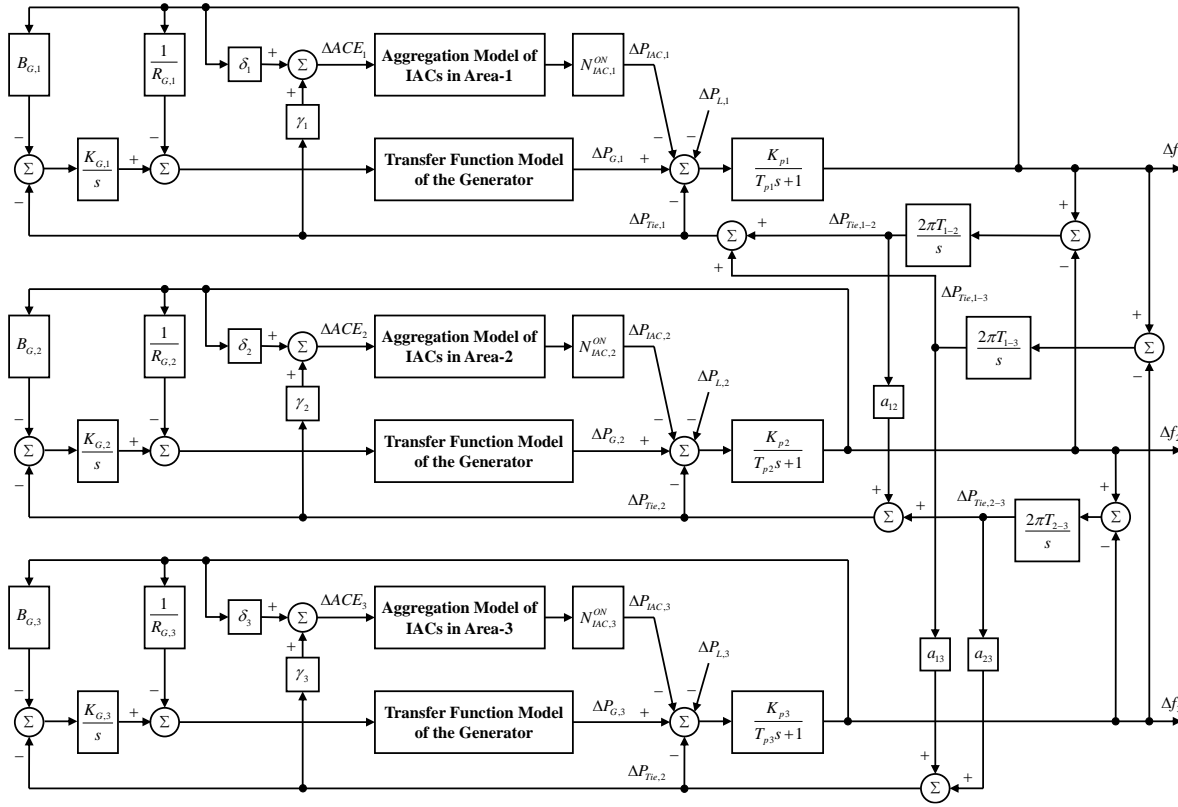


Fig. 6. The transfer function model of the three-area power systems with IACs participating in regulation services.

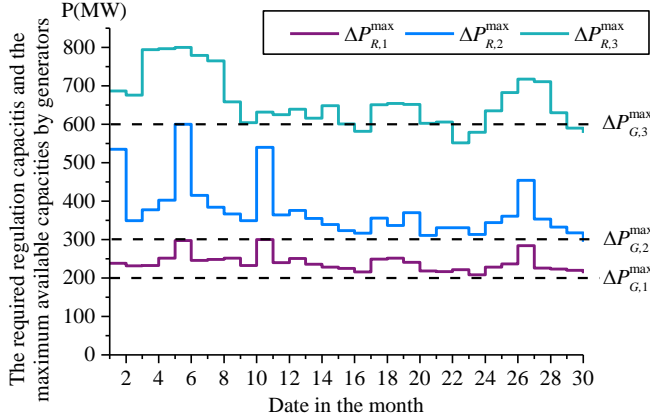


Fig. 7. The required regulation capacity of the power system and the maximum regulation capacity provided by generators.

operation period of the power system in real time, the remaining action number of IACs  $RANC_{IAC,k}(t)$  should be updated after the occurrence of the disturbance power. Then the IACs will be ranked again and another batch of frontal IACs will be selected.

When the day is over,  $\Delta P_{R,i}^{\max}(t)$  and  $\Delta P_{G,i}^{\max}(t)$  of the last days in the month can be modified based on the updating load forecasting. The allocated action number of IACs on each day should also be updated based on the remaining action number of IACs. Therefore, the Equation (21) should be replaced by:

$$N_{IAC}^{\max}(t) = \sum_{i \in N_i} \sum_{k \in N_i} RANC_{IAC,k}(t) \cdot P_{SHT}(t) / \sum_{i \in D} P_{SHT}(t) \quad (32)$$

The scheduling model will end when the month is over, as shown in Fig. 5.

## V. CASE STUDIES

### A. The Test System

The test system adopts the three-area power systems as the studies in [19], [20], as shown in Fig. 6. The rated frequency of the power system is 50Hz, and the rated capacities of the three-area power systems are  $P_{r,1}=2,000\text{MW}$ ,  $P_{r,2}=4,000\text{MW}$  and  $P_{r,3}=8,000\text{MW}$ , respectively. The inertia time constants and damping factors of the three-area power systems are  $T_{p,1}=T_{p,2}=T_{p,3}=20\text{s}$  and  $K_{p,1}=K_{p,2}=K_{p,3}=100\text{Hz/p.u.}$ , respectively. The tie line time constants of the three-area power systems are  $T_{1-2}=T_{1-3}=T_{2-3}=0.544\text{s}$ . Moreover, the parameters of the reheat steam governors in the three-area power systems are set as  $T_{g,1}=T_{g,2}=T_{g,3}=0.08\text{s}$ ,  $T_{t,1}=T_{t,2}=T_{t,3}=0.3\text{s}$ ,  $T_{r,1}=T_{r,2}=T_{r,3}=10\text{s}$ ,  $F_{HP,1}=F_{HP,2}=F_{HP,3}=0.5$  and  $R_{G,1}=R_{G,2}=R_{G,3}=4$ . The required regulation capacity  $\Delta P_{R,i}^{\max}(t)$  and the maximum regulation capacity of the generators  $\Delta P_{G,i}^{\max}(t)$  come from the real power systems' data in 2017, in Jiangsu Province, China, as shown in Fig. 7.

The parameters of the thermal and electric model of IACs are from the national standards of China [2], which are set as  $\rho_A=1.205\text{kg/m}^3$ ,  $c_A=1.005\text{kJ/kg}^\circ\text{C}$ ,  $\xi=0.5\text{h}^{-1}$ ,  $U_{HT}=3.6\text{W/m}^3\text{^\circ C}$ ,  $Q_{dis}=0.43\text{kW}$ ,  $V=250\text{m}^3$ ,  $A_S=300\text{m}^2$ ,  $\kappa_P=0.04\text{kW/Hz}$ ,  $\mu_P=0.02\text{kW}$ ,  $\kappa_Q=0.12\text{kW/Hz}$ ,  $\mu_Q=-0.05\text{kW}$ ,  $f_c^{\min}=1\text{Hz}$ ,  $f_c^{\max}=150\text{Hz}$ ,  $\theta=0.52\text{Hz}/^\circ\text{C}$ ,  $\eta=0.032\text{Hz}/^\circ\text{C/s}$ ,  $\beta=0.01$ ,  $T_{set}=24^\circ\text{C}$ ,  $\Delta T_A^{\min}=-1^\circ\text{C}$ ,  $\Delta T_A^{\max}=1^\circ\text{C}$ , and  $T_0=33^\circ\text{C}$ . Moreover, the rate limitation of the IAC compressor is 10Hz/s. The maximum number of the available IACs in the multi-area system are assumed to be 200,000, which accounts for around 5% of the total capacity of

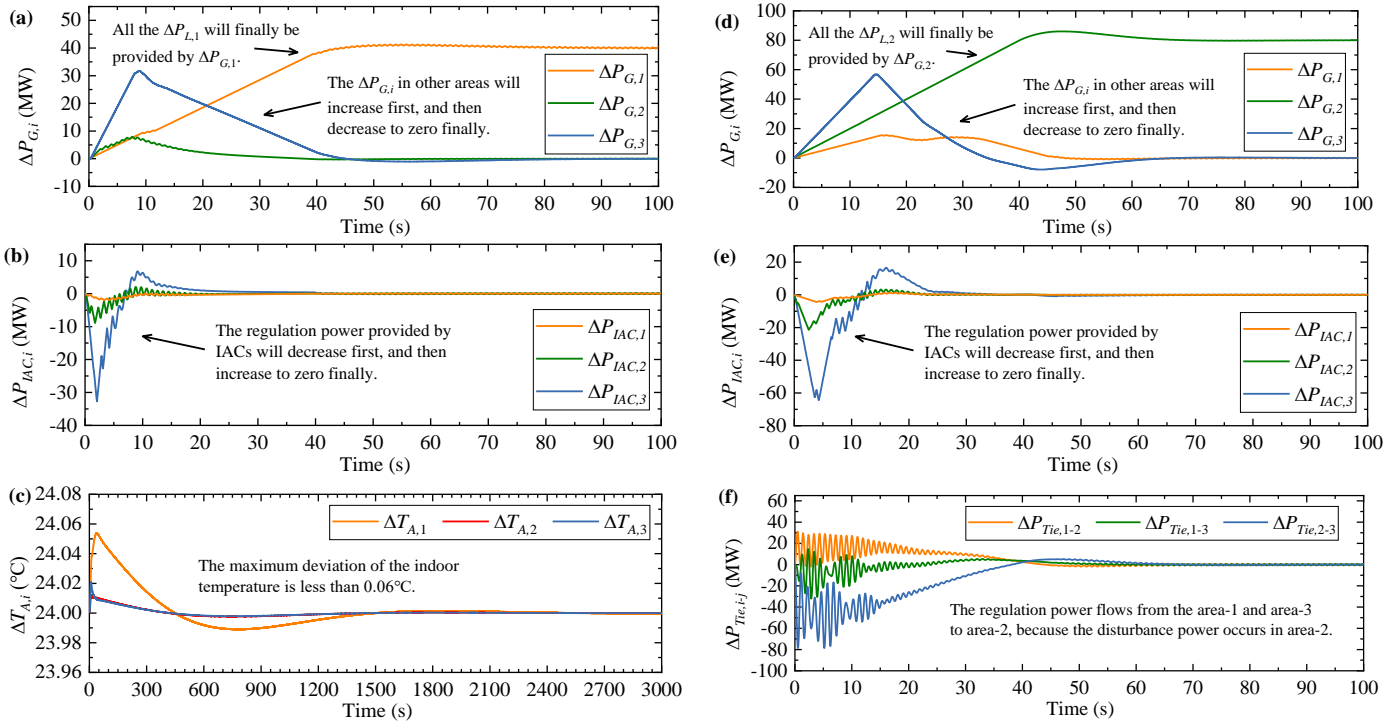


Fig. 8. The simulation results in real time in Case 1. (a) The regulation power of generators when the disturbance power occurs in area 1. (b) The regulation power of IACs when the disturbance power occurs in area 1. (c) The indoor temperature fluctuations when the disturbance power occurs in area 1. (d) The regulation power of generators when the disturbance power occurs in area 2. (e) The regulation power of IACs when the disturbance power occurs in area 2. (f) The tie line power deviations when the disturbance power occurs in area 2.

the power system. The maximum action number of each IAC is five times, and the available time of each IAC is allocated randomly in the days of the month.

#### B. Regulation Capacity Allocation and Control Parameter Optimization of IACs

Based on the Equations (21)-(23), the regulation capacity provided by IACs can be allocated among the days before the beginning of the month, which are shown in Table I.

TABLE I.  
THE REGULATION CAPACITY ALLOCATION RESULTS OF IACS

| Date | $N_{IAC}^{\max}$ | Date | $N_{IAC}^{\max}$ | Date | $N_{IAC}^{\max}$ | Date | $N_{IAC}^{\max}$ |
|------|------------------|------|------------------|------|------------------|------|------------------|
| 1    | 70,252           | 9    | 16,806           | 17   | 30,365           | 25   | 35,146           |
| 2    | 30,453           | 10   | 72,638           | 18   | 27,826           | 26   | 69,431           |
| 3    | 59,402           | 11   | 25,149           | 19   | 31,770           | 27   | 37,060           |
| 4    | 68,587           | 12   | 32,353           | 20   | 6,116            | 28   | 16,683           |
| 5    | 116,745          | 13   | 20,886           | 21   | 10,492           | 29   | 5,452            |
| 6    | 66,513           | 14   | 22,720           | 22   | 774              | 30   | 0                |
| 7    | 58,245           | 15   | 9,640            | 23   | 170              | -    | -                |
| 8    | 34,563           | 16   | 2,770            | 24   | 21,006           | -    | -                |

It can be seen that more IACs will be scheduled when the regulation capacity provided by generators is insufficient, for example, 116,745 IACs are allocated on the 5th day. However, the allocated IACs will be less or even equal to zero if the regulation capacity of generators is enough, such the thirty day.

Based on the total available number of IACs on one day, the IACs among areas can be allocated from the optimization model (24)-(30). Three disturbance power scenarios are assumed to occur in the multi-area power systems, i.e., 2% of the rated capacity ( $\Delta P_{L,1} = 40\text{MW}$ ,  $\Delta P_{L,2} = 80\text{MW}$ , and

$\Delta P_{L,3} = 160\text{MW}$ ), respectively. The first day is taken as an example, when there are 70,252 IACs participate in the regulation service. The maximum available IACs in each area on this day are 15,000, 30,000 and 60,000, respectively. The optimization model is solved by the particle swarm optimization algorithm [26], [27], in which the parameters are set as: iteration number is 50; swarm number is 50; adjustment coefficients of the initial vector, group best vector and individual best vector are 0.8, 2.5 and 1.5, respectively.

The system is formulated in MATLAB R2014a, on a laptop with Intel(R) Core(TM) i7-5500U processors, clocking at 2.40GHz and 8GB RAM. It takes 1301.359 seconds (i.e., around 22 minutes) to calculate the parameters, as shown in Table II (Case 1). This calculation process is before the beginning of the day, which will not affect the controllers' response time in real time.

In the same case, the differences of the control parameters in different areas are mainly related to two reasons. The first one is the different characteristics of the generators in different areas, which have huge gaps in the capacities and can lead to different control parameters for the generators. The second reason is the different number of IACs in the three areas. These IACs can provide regulation services for both themselves' areas and the other areas to minimize the ACE of the multi-area power systems, which cause different control parameters for IACs. For example, the number of IACs in area-3 is the largest, so that  $\gamma_3$  is larger than  $\gamma_1$  and  $\gamma_2$  to realize more regulation functions for area-1 and area-2. Moreover,  $\gamma_2$  is 4.216, which is the smallest among the three values. It indicates that the IACs in area-2 should decrease the regulation services' interaction

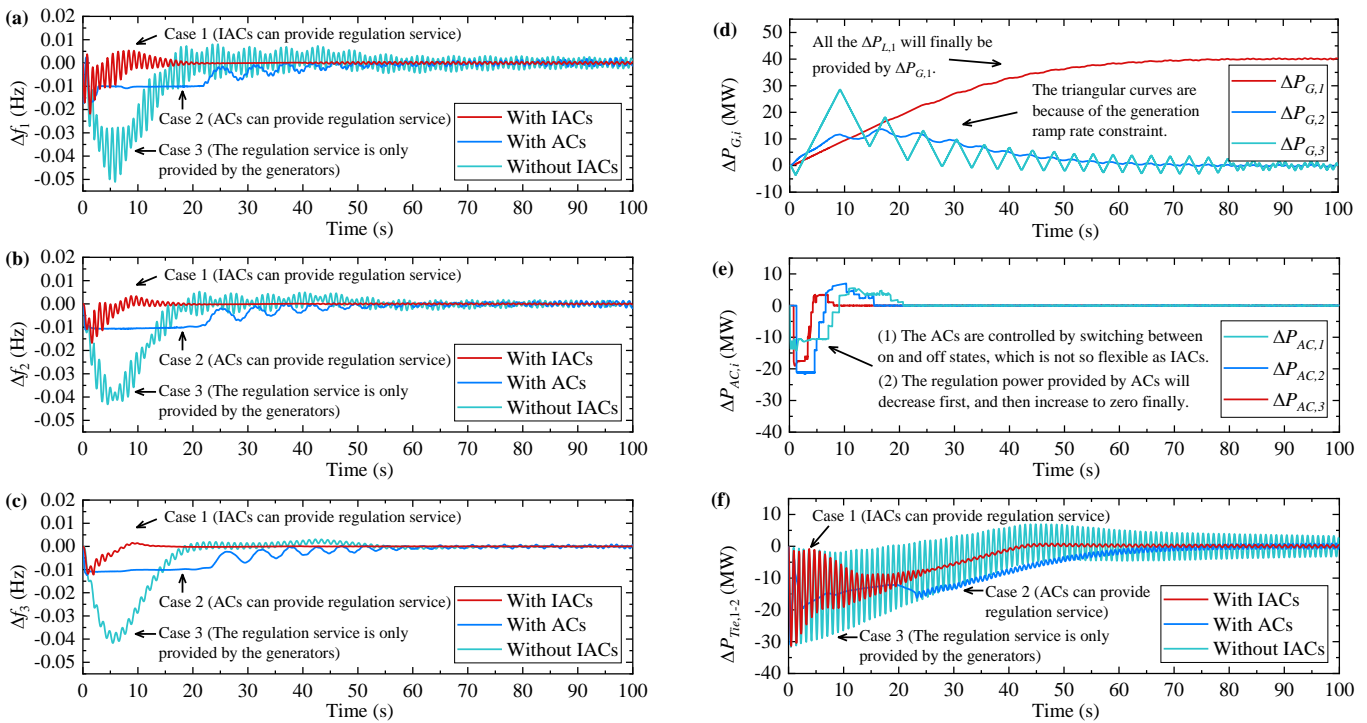


Fig. 9. The comparisons of the frequency regulation effects among the three cases when the disturbance power occurs in area 1. (a) The frequency deviations in area 1. (b) The frequency deviations in area 2. (c) The frequency deviations in area 3. (d) The regulation power of generators in case 2. (e) The regulation power of ACs in case 2. (f) The tie line power deviations between area 1 and area 2.

with area-1 and area-3, in order to realize the optimization objective, i.e., minimize the total ACE of the multi-area power systems.

TABLE II

THE OPTIMIZATION RESULTS OF THE ALLOCATED CAPACITIES AND CONTROL PARAMETERS IN THE MULTI-AREA POWER SYSTEMS

| Case   | Area | $B_{G,i}$ | $K_{G,i}$ | $\delta_i$ | $\gamma_i$ | $N_{IAC,i}^{\max}(t)$ |
|--------|------|-----------|-----------|------------|------------|-----------------------|
| Case 1 | 1    | 90.023    | 1.8501    | 2,054      | 219.8      | 2,849                 |
|        | 2    | 1.4732    | 0.2180    | 689        | 4.216      | 22,126                |
|        | 3    | 4.6119    | 0.1708    | 1,691      | 390.6      | 45,098                |
| Case 2 | 1    | 98.003    | 0.0017    | 10000      | 3.6148     | 14,998                |
|        | 2    | 0.6990    | 0.1149    | 9918       | 977.80     | 30,000                |
|        | 3    | 0.3221    | 9.9870    | 9312       | 1001.4     | 25,014                |
| Case 3 | 1    | 0.1154    | 0.4964    | -          | -          | -                     |
|        | 2    | 0.3209    | 0.0903    | -          | -          | -                     |
|        | 3    | 0.3511    | 0.0639    | -          | -          | -                     |

### C. Control of IACs in Real Time

Based on the optimization results in Table II, there are 2,849, 22126 and 45098 IACs selected in area-1, area-2 and area-3, respectively. The corresponding control parameters  $\delta_i$  and  $\gamma_i$  are set to the selected IACs. Besides, the control parameters  $B_{G,i}$  and  $K_{G,i}$  are set to the generators in each area.

It is assumed that 40MW disturbance power occurs in area-1 in real time, when the generators and IACs in each area will take action to change operating states and provide regulation power. The simulation results are shown in Fig. 8(a)-(c). Fig. 8(a) shows the regulation power of the generators in Case 1. It can be seen that all the generators will increase the power generation when the disturbance power occurs. The generator in area 1 will finally provide all the additional load power, while the generators in other areas will recover to the

original operating state at the end of the regulation. Similarly, if the disturbance power occurs in area-2 in real time ( $\Delta P_{L,2}=80\text{MW}$ ), all the generators will also increase the power generation and the generator in area 2 will finally provide all the additional load power, as shown in Fig. 8(d).

By contrast, as shown in Fig. 8(b) and Fig. 8(e), the IACs in Case 1 will decrease the power consumption as soon as the disturbance power occurs. In this manner, the IACs can achieve the same effect with the generators on assisting the power system to recover balance. Moreover, it can be seen that the IACs' power can be regulated more rapidly than the generators' power. The faster regulation speed is useful for the reduction of the system frequency deviations. The IACs mainly contribute to the regulation services in the first 20 seconds, and phase out when the power system recovers the steady state. Because the changed operating frequency and power consumption can lead to the appearance of the temperature deviation, i.e., the  $T_{dev}$  is not zero any more. The temperature deviation will cause the reverse regulation of the compressor's operating frequency. Therefore, the IACs seem to phase out when the power system return to the steady state. It is a beneficial control strategy for both providing regulation services to the power systems and guaranteeing the customers' comfort. Besides, it can be seen from Fig. 8(b) and Fig. 8(e) that the IACs' power exceed the original operating power value temporarily in the process of recovery, i.e., the  $\Delta P_{IAC,i}$  is larger than zero slightly in the recovery procedure. This is because the indoor temperatures are affected when the IACs provide operating reserve, and the IACs have to consume more energy to restore the indoor temperatures along with the recovery of the system balance.

Fig. 8(c) shows the indoor temperature fluctuations in Case

1. The original indoor temperature is 24°C and the maximum temperature deviation is less than 24.06°C. Finally, the indoor temperature returns to the set point around 25min later. Therefore, the indoor temperature can be guaranteed in the allowable ranges and will return to the set temperature as soon as the finish of the regulation process. The temperature deviation process is slower than other deviation processes, such as the power system frequency deviations and power consumption deviations. Because the power consumption can be regulated rapidly by adjusting the compressor's operating frequency within 20s. However, the influence due to the power consumption adjustment cannot be reflected on the indoor temperature in such a short time period. The room has thermal insulation function, i.e., the specific heat ratio in equations (1)-(2). Therefore, the indoor temperature deviation process is slower than the power consumption deviation process.

Fig. 8(f) shows the tie line power deviations when the disturbance power occurs in area-2. The  $\Delta P_{Tie,1-2}$  is positive while the  $\Delta P_{Tie,2-3}$  is negative, which indicate that the regulation power flows from the area-1 and area-3 to area-2. That is to say, the other areas can provide regulation services to the disturbance power area to assist the multi-area power systems to recover balance. Besides, the  $\Delta P_{Tie,1-3}$  fluctuates around zero and the values are smaller than  $\Delta P_{Tie,1-2}$  and  $\Delta P_{Tie,2-3}$ . Because the area-1 and area-3 have no disturbance in this case, and do not need to adjust the tie line power to provide regulation power to each other.

#### D. Comparison of Frequency Regulation Effects Among the Three Systems with IACs, without IACs, and with Regular ACs

In order to compare the regulation effects on the power system before and after considering IACs, another two cases are considered: the ACs can provide regulation service by *on/off* control method in Case 2 [9], [11], [12], [20]; no IAC or AC provide regulation service in Case 3 [18], [19]. It is assumed that the operating capacities provided by ACs in Case 2 are the same with that by IACs in Case 1. Besides, the control parameters of the generators and ACs in Case 2 and Case 3 are also obtained by the optimization model. The results are shown in Table II. In different cases, the differences of the control parameters are mainly related to the architectures of the multi-area power systems. The different system architectures and different kinds of flexible loads cause different control parameters. For example, the control parameters ( $\delta_i$  and  $\gamma_i$ ) are for IACs in case 1, for ACs in case 2, and not applicable in case 3.

Fig. 9(a)-(c) show the frequency deviations in the three cases. It can be seen that the system frequency will drop rapidly and then increase gradually under the regulation of the generators and IACs. The frequency deviations in Case 1 can recover to the rated value faster than that in Case 3, which proofs that IACs can keep down the frequency deviations by providing regulation service. The maximum system frequency deviation in Case 1 is -0.022 Hz, while it is -0.053 Hz in Case 3. The main reason is that the IACs can take action and provide regulation power faster than the generators, so that the gap between the disturbance power and generation power can be

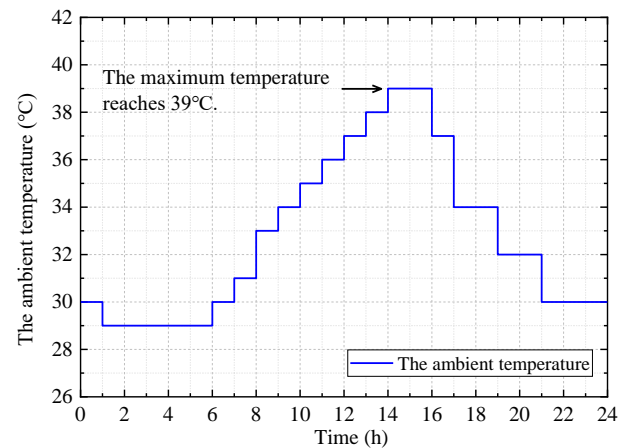


Fig. 10. The ambient/outdoor temperature in Jiangsu Province, China, on Aug. 7<sup>th</sup>, 2017 [28].

decrease rapidly in a short time. It can also be proved from the tie line power deviations in Fig. 9(f), where the maximum tie line power deviations in the two cases are similar, while the recovery time is the shortest in Case 1 (with IACs), and the longest in Case 3 (without IACs). Consequently, the IACs can provide operating reserve for the power system, which contributes to the decrease of the frequency deviations, the tie line power deviations, and the recovery time.

The comparisons of the regulation services provided by IACs and ACs are also shown in Fig. 9. The frequency deviations in Case 2 are decreased compared with that in Case 3, due to the regulation capacities of ACs, as shown in Fig. 9(a)-(c). However, compared with Case 1, the recovery time of the system frequency is longer in Case 2, and the system frequency shows more oscillations during the recovery process. Because the ACs can only switch between *on* and *off* states, the control methods of ACs cannot be so flexible as IACs. The comparisons of the regulation power provided by the IACs and ACs are shown in Fig. 8(b) and Fig. 9(e), respectively. The IACs can change the compressors' operating frequency to adjust the power consumption, which is fast and suitable for varying degrees of frequency deviations. While as for regular ACs, the *on/off* control methods in [9], [11], [12], [20] have to set the response thresholds of the deviations, in order to avoid the frequent switch between *on* and *off* states. Therefore, the ACs cannot take action if the frequency deviation is less than the minimum value of the thresholds. Besides, the ACs may be damaged if they are shut down suddenly too many times. Therefore, regular ACs can indeed provide regulation service for the power system, while they are not suitable to change the operating states in a short time and cannot provide frequency regulation services so good as IACs.

#### E. Simulation Results Over Several Hours Considering Both Up and Down Regulation Services

In order to verify the effectiveness of the regulation services provided by the generators and IACs over a long period of time, the simulation is carried out for six hours (10:00-16:00) considering both up and down regulations (Case 4). Moreover, the outdoor temperature is also considered in the simulation,

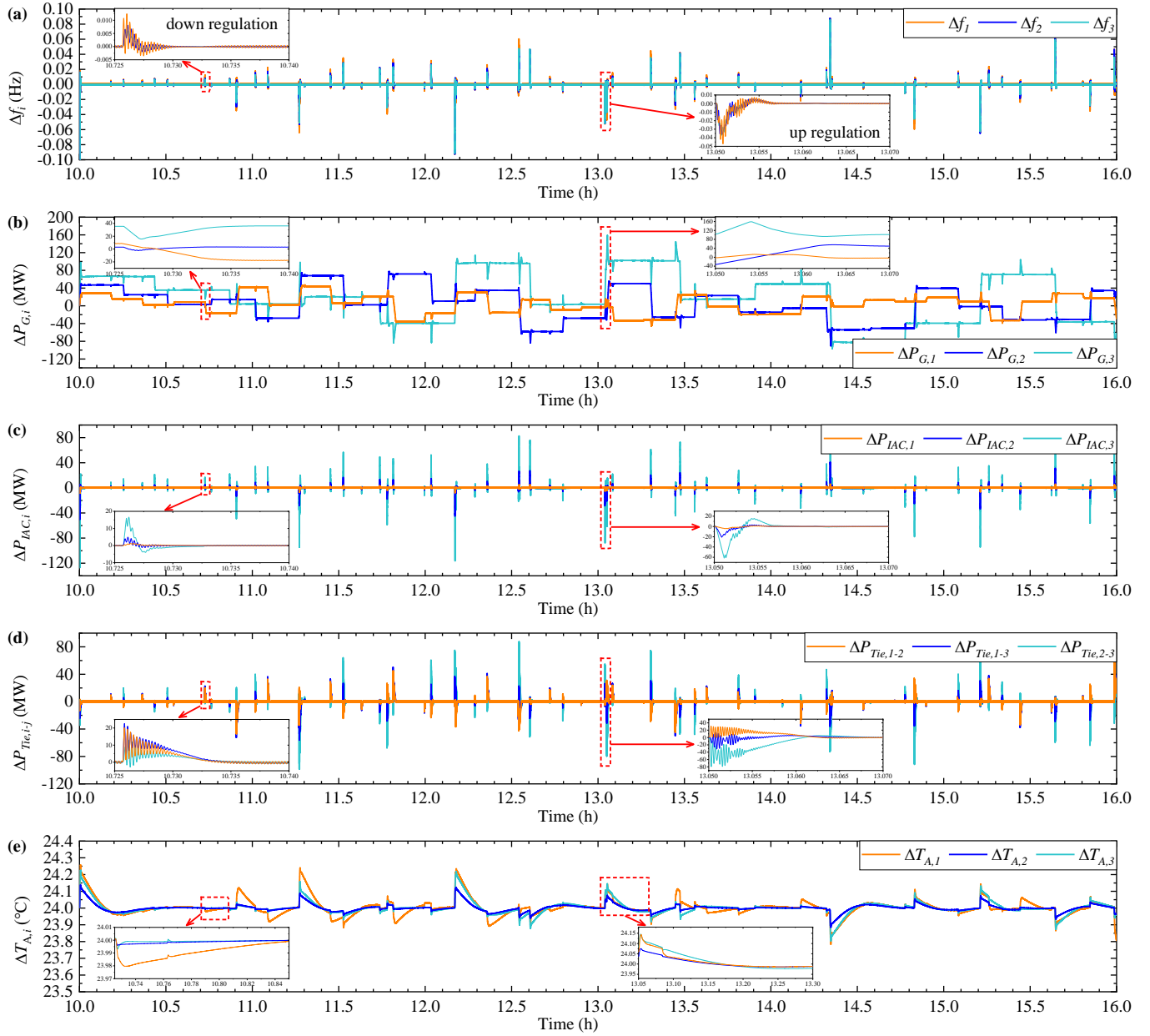


Fig. 11. The simulation results in real time in Case 4 (last for 6 hours from 10:00 to 16:00). (a) The frequency deviations. (b) The regulation power of generators. (c) The regulation power of IACs. (d) The tie line power deviations. (e) The indoor temperature fluctuations.

which is based on the real ambient temperature in Jiangsu Province, China, on August 7th, 2017, as shown in Fig. 10 [28]. The disturbance power values are assumed to obey the normal distribution by using the mean value zero and the standard deviation 2%. Therefore, the generators and IACs have to provide both up and down regulation services. Besides, the disturbance power is assumed to occur randomly among the areas in the three-area power systems. The other parameters are set to be the same as that in Case 1.

The simulation results are shown in Fig. 11, which includes the system frequency deviations, the regulation power provided by generators and IACs, the tie line power deviations, and the indoor temperature fluctuations. There are many spikes in Fig. 11, because this figure shows the deviations for six hours, while the AGC performance makes the deviations return to the

objective values within only around 30s. The fluctuations cannot be presented as detailed as that in Fig. 8 and Fig. 9.

In order to show more specifics, two spikes in Fig. 11 are amplified to show the curves' details, i.e., the down regulation service at 10:43:30 and the up regulation service at 13:03:00. It can be seen that the system frequencies in Fig. 11(a) can be stabilized to zero under the regulation services provided by the generators in Fig. 11(b) and the IACs in Fig. 11(c). Here the IACs can provide down regulation services, i.e., increasing the power consumption. Because the operating power of IACs can be regulated flexibly by adjusting the operating frequency of the compressor. Generally, when the IAC is just turned on, the operating frequency of the compressor is high to make the indoor temperature reach the set point as soon as possible. However, the operating frequency will reduce to a steady value

when the indoor temperature reaches the set temperature. That is to say, the operating frequency will not be in the maximum value at most of the operating time, when the IACs are in the steady state. Therefore, as for the aggregation of IACs, most of the IACs have the capability to provide both up and down regulation services. Only a small part of IACs, which are just turned on, may have no capability to increase the power consumption and provide the down regulation service. Moreover, in reality, the down regulation service by IACs is uncommon when the outdoor temperature is high. Because the power consumption is large in the high temperature moment, which may lead to all the available generators working at full capacity. The up regulation capacity (i.e., increasing the power generation of generators) will be short for dealing with the sudden positive disturbance power. Therefore, the pressing need is to provide equivalent up regulation capacity by cutting down the power consumption of IACs. At this moment, the down regulation capacity (i.e., decreasing the power generation of generators) is generally ample, because the generators have been working at full capacity and hope to decrease the power generation.

Besides, the indoor temperature fluctuations are shown in Fig. 11(e), where the minimum and maximum temperature deviations are  $23.75^{\circ}\text{C}$  and  $24.25^{\circ}\text{C}$ , respectively. Therefore, the indoor temperature can also be guaranteed in the allowable ranges.

#### F. Discussions

The proposed modelling and scheduling methods in this paper show huge potential of IACs to provide regulation services for the power systems. In fact, the progressed information and communication technologies have made it easier and lower cost to build the instant communication system nowadays. For example, in USA, the Lawrence Berkeley National Laboratory created a standard for implementing DR, i.e., OpenADR [29]. The entire interaction can be realized over the existing internet connection and completed in milliseconds. The OpenADR 2.0 has included the fast response services, such as frequency regulation services for the power systems [30]. In Europe, such as Denmark, some field experiments have verified that the fast frequency regulation services can be provided by bottle cooling refrigerators, the electric space heaters and wastewater treatment plants [31]. Besides, several DR projects had been implemented in Romania, including the installation of advanced metering management systems to households with fiber optics and GPRS, and the installation of power line communication system to small economic operators [32]. In China, the *State Grid Corporation of China* implemented the *Large-scale Source-Grid-Load Friendly Interactive System* project to realize the rapid control of loads on the time scale of milliseconds to avoid the sharp drop of the system frequency caused by the failure of the Ultra High Voltage Direct Current transmission line [33], where around 2,600MW loads have been connected to the optical fiber communication network [34]. Besides, the *Control System Reformation of Air Conditioning Systems in Public Buildings* project reformed the IACs to realize the flexible regulation of

the compressors' operating frequency. On this basis, the IACs can provide frequency regulation services or reduce the peak loads during hot days in summer.

Moreover, the cyber-security is also concerned in these projects. For example, there are two types of communication systems for the power systems' operation in China. One is by the name of the private network, and the other one is named extranet. The control signals and data monitoring of loads in DR projects are based on the private network. Only some information (e.g., electricity bills and DR bonuses) is released via the extranet. In this way, the communication systems for the power systems can realize the physical isolation with the extranet, to ensure the security of customers' data. Therefore, the instant two way communication system will be available more widely in the near future, which is precisely the scenario that this paper focuses on.

## VI. CONCLUSIONS

This paper presents a novel frequency regulation model of multi-area power systems considering regulation service provided by large-scale IACs. Based on the proposed thermal and electric model of IACs, the control strategy and available capacities of IACs in the multi-area power system are analyzed and quantified. Moreover, the scheduling model for allocating the regulation capacities of IACs among the days in the month is developed, and in which the optimization model of the IACs' control parameters is proposed for minimizing the ACE of the multi-area power systems. Illustrative results show that the system frequency deviations and tie line power deviations can be kept down when IACs participate in the regulation service, in which the customers desired indoor temperature can also be guaranteed. The comparison results in the case studies between IACs and regular ACs also show that IACs are more suitable to provide frequency regulation service than ACs.

## ACKNOWLEDGMENT

The authors would like to thank all the editors and reviewers for providing valuable comments to improve the quality of this paper. The suggestions on the proposed control strategy of IACs and the supplementation of case studies are greatly appreciated.

## REFERENCES

- [1] A Record High of Power Grid Load in Beijing, Beijing Daily, 2017. [Online]. Available: <http://www.chinanews.com/kong/2017/07-13/827645.shtml>
- [2] H. Hui, Y. Ding, W. Liu, Y. Lin and Y. Song, "Operating reserve evaluation of aggregated air conditioners," *Appl. Energy*, vol. 196, pp. 218-228, Jun. 2017.
- [3] *Administrative Investigation Report on the Power Failure 815*, Executive Yuan, Taiwan, China, Technical Report, 2017. [Online]. Available: <http://www.ey.gov.tw>
- [4] H. Hui, Y. Ding, K. Luan and D. Xu, "Analysis of 815 blackout in Taiwan and the improvement method of contingency reserve capacity through direct load control," 2018 *IEEE Power & Energy Society General Meeting, IEEE*, 2018.
- [5] J. Wang, X. Wang and Y. Wu, "Operating reserve model in the power market," *IEEE Trans. Power Syst.*, vol. 20, no. 1, pp. 223-229, Feb. 2005.
- [6] M. A. Ortega-Vazquez and D. S. Kirschen, "Optimizing the spinning reserve requirements using a cost/benefit analysis," *IEEE Trans. Power*

- Syst.*, vol. 22, no. 1, pp. 24-33, Feb. 2007.
- [7] Q. Shi, F. Li, Q. Hu, and Z. Wang, "Dynamic demand control for system frequency regulation: concept review, algorithm comparison, and future vision," *Electr. Power Syst. Res.*, vol. 154, pp. 75-87, Jan. 2018.
- [8] P. Siano, "Demand response and smart grids—A survey," *Renew. Sustain. Energy Rev.*, vol. 30, pp. 461-478, Feb. 2014.
- [9] Q. Hu, F. Li, X. Fang and L. Bai, "A framework of residential demand aggregation with financial incentives," *IEEE Trans. Smart Grid*, vol. 9, no. 1, pp. 497-505, Jan. 2018.
- [10] Y. Ding, S. Pineda, P. Nyeng, J. Østergaard, E. M. Larsen, and Q. Wu, "Real-time market concept architecture for EcoGrid EU—A prototype for European smart grids," *IEEE Trans. Smart Grid*, vol. 4, no. 4, pp. 2006-2016, Dec. 2013.
- [11] Q. Hu and F. Li, "Hardware design of smart home energy management system with dynamic price response," *IEEE Trans. Smart Grid*, vol. 4, no. 4, pp. 1878-87, Dec. 2013.
- [12] N. Lu, "An evaluation of the HVAC load potential for providing load balancing service," *IEEE Trans. Smart Grid*, vol. 3, no. 3, pp. 1263-1270, Sep. 2012.
- [13] W. Cui, Y. Ding, H. Hui, Z. Lin, P. Du, Y. Song and C. Shao, "Evaluation and sequential dispatch of operating reserve provided by air conditioners considering lead-lag rebound effect," *IEEE Trans. Power Syst.*, vol. 33, no. 6, pp. 6935-50, Nov. 2018.
- [14] Q. Shi, F. Li, G. Liu, D. Shi, Z. Yi, and Z. Wang, "Thermostatic load control for system frequency regulation considering daily demand profile and progressive recovery," *IEEE Trans. Smart Grid*, in press.
- [15] P. Siano and D. Sarno, "Assessing the benefits of residential demand response in a real time distribution energy market," *Appl. Energy*, vol. 161, pp. 533-551, Jan. 2016.
- [16] *What is inverter technology air conditioner*, Bijli Bachao, 2017. [Online]. Available: <https://www.bijlibachao.com>
- [17] *The market share of inverter air conditioners rises to 54.06%*, China Household Appliance Network, 2011. [Online]. Available: <http://app.cheaa.com/readnews.php?contentid=295609>
- [18] M. L. Kothari, J. Nanda, D. P. Kothari and D. Das, "Discrete-mode automatic generation control of a two-area reheat thermal system with new area control error," *IEEE Trans. Power Syst.*, vol. 4, no. 2, pp. 730-738, May 1989.
- [19] J. Nanda, S. Mishra and L. C. Saikia, "Maiden application of bacterial foraging-based optimization technique in multiarea automatic generation control," *IEEE Trans. Power Syst.*, vol. 24, no. 2, pp. 602-609, May 2009.
- [20] Y. Bao, Y. Li, B. Wang, M. Hu and P. Chen, "Demand response for frequency control of multi-area power system," *Journal of Modern Power Syst. and Clean Energy*, vol. 5, no. 1, pp. 20-29, Jan. 2017.
- [21] B. Pouya, Q. Shafee and H. Bevrani, "Intelligent demand response contribution in frequency control of multi-area power systems," *IEEE Trans. Smart Grid*, vol. 9, no. 2, pp. 1282-1291, March 2018.
- [22] S. Shao, W. Shi, X. Li and H. Chen, "Performance representation of variable-speed compressor for inverter air conditioners based on experimental data," *Int. Journ. Refrig.*, vol. 27, no. 8, pp. 805-815, Dec. 2004.
- [23] N. Lu and D. P. Chassin, "A state-queueing model of thermostatically controlled appliances," *IEEE Trans. Power Syst.*, vol. 19, no. 3, pp. 1666-1673, Aug. 2004.
- [24] H. Hui, Y. Ding and M. Zheng, "Equivalent modeling of inverter air conditioners for providing frequency regulation service," *IEEE Trans. Ind. Electron.*, vol. 66, no. 2, pp. 1413-1423, Feb. 2019.
- [25] Q. Shi, H. Cui, F. Li, Y. Liu, W. Ju and Y. Sun, "A hybrid dynamic demand control strategy for power system frequency regulation," *CSEE Journ. Power and Energy Syst.*, vol. 3, no. 2, pp. 176-185, Jun. 2017.
- [26] M. Clerc and J. Kennedy, "The particle swarm-explosion, stability, and convergence in a multidimensional complex space," *IEEE Trans. Evolutionary Computation*, vol. 6, no. 1, pp. 58-73, Feb. 2002.
- [27] L. Abdul, D. C. Das, S. Ranjan and I. Hussain, "Integrated demand side management and generation control for frequency control of a microgrid using PSO and FA based controller," *Intern. Journ. Renew. Energy Res.*, vol. 8, no. 1, pp. 188-199, Mar. 2018.
- [28] *The Ambient Temperature on August 7<sup>th</sup>, 2017, in Nanjing, Jiangsu Province, China*, Weather Underground, 2017. [Online]. Available: <https://www.wunderground.com/history/daily/cn/nanjing/ZSNJ/date/2017-8-7>
- [29] *OpenADR*. [Online]. Available: <https://www.openadr.org/>
- [30] *OpenADR: Success stories*. [Online]. [https://www.openadr.org/assets/docs/openadr\\_regen\\_v3.pdf](https://www.openadr.org/assets/docs/openadr_regen_v3.pdf)
- [31] P. J. Douglass, R. Garcia-Valle, P. Nyeng, J. Østergaard and M. Togeby, "Smart demand for frequency regulation: Experimental results," *IEEE Trans. Smart Grid*, vol. 4, no. 3, pp. 1713-20, Sep. 2013.
- [32] *Demand Response Status in EU Member States*, EU Science Hub, 2016. [Online]. Available: <https://ec.europa.eu/jrc/en/publication/eur-scientific-and-technical-research-reports/demand-response-status-eu-member-states>
- [33] J. Yao, S. Yang, K. Wang, Z. Yang and X. Song, "Concept and research framework of smart grid Source-Grid-Load interactive operation and control," *Autom. of Electr. Power Syst.*, vol. 21, pp. 1-6, 12, 2012.
- [34] *The first source-grid-load system in China*, Energy News, 2018. [Online]. Available: <http://www.in-en.com/article/html/energy-2271035.shtml>

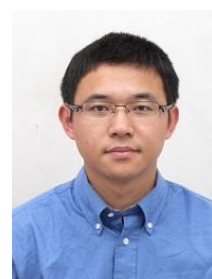


**Hongxun Hui** (S'17) received the bachelor's degree in electrical engineering from Zhejiang University, Hangzhou, China in 2015, where is currently working toward the Ph.D. degree in electrical engineering. He was elected in the first batch of the Academic Rising Star Program in Zhejiang University in 2018. His research interests include modelling and optimal control of demand side resources

in smart grid, the electricity market considering demand response, and the uncertainty analysis brought by flexible loads and renewable energies.



**Yi Ding** (M'12) received the bachelor's and Ph.D. degrees in electrical engineering from Shanghai Jiaotong University, Shanghai, China, and Nanyang Technological University, Singapore in 2000 and 2007, respectively. He is a Professor with the College of Electrical Engineering, Zhejiang University, Hangzhou, China. His current research interests include power systems reliability/performance analysis incorporating renewable energy resources, smart grid performance analysis, and engineering systems reliability modeling and optimization.



**Zhenzhi Lin** received the Ph.D. degree in electrical engineering from South China University of Technology, Guangzhou, China, in 2008.

He was a Research Assistant in the Department of Electrical Engineering at The Hong Kong Polytechnic University from 2007 to 2008, a Research Scholar in the Min Kao Department of Electrical Engineering and Computer Science at the University of Tennessee from 2010 to 2011, and a Research Associate in College of Engineering and Computing Sciences at Durham University from 2013 to 2014. He is currently an Associate Professor in the College of Electrical Engineering, Zhejiang University, Hangzhou, China.

His research interests include power system wide-area monitoring and control, big data analysis and power system restoration.



**Pierluigi Siano** (M'09-SM'14) received the M.Sc. degree in electronic engineering and the Ph.D. degree in information and electrical engineering from the University of Salerno, Salerno, Italy, in 2001 and 2006, respectively.

He is a Professor and Scientific Director of the Smart Grids and Smart Cities Laboratory with the Department of Management & Innovation Systems, University of Salerno. His research activities are centered on demand response, on the integration of distributed energy resources in smart grids and on planning and management of power systems.

He has co-authored more than 420 papers including more than 200 international journal papers that received more than 6600 citations with an H-index equal to 43. He has been the Chair of the IES TC on Smart Grids. He is an Associate Editor of the IEEE TRANSACTIONS ON INDUSTRIAL INFORMATICS, of the IEEE TRANSACTIONS ON INDUSTRIAL ELECTRONICS and of IET Renewable Power Generation.



**Yonghua Song** (M'90-SM'94-F'08) received the B.Eng. and Ph.D. degrees from Chengdu University of Science and Technology, Chengdu, China, and China Electric Power Research Institute, Beijing, China, in 1984 and 1989, respectively.

He is the President of University of Macau, and also an Adjunct Professor at College of Electrical Engineering, Zhejiang University and Department of Electrical Engineering, Tsinghua University. From 1989 to 1991, he was a Post-Doctoral Fellow with Tsinghua University, Beijing. He then held various positions at Bristol University, Bristol, U.K.; Bath University, Bath, U.K.; and John Moores University, Liverpool, U.K., from 1991 to 1996. In 1997, he was a Professor of power systems with Brunel University, Uxbridge, U.K., where he has been the Pro-Vice Chancellor of Graduate Studies since 2004. In 2007, he took up the Pro-Vice Chancellorship and Professorship of Electrical Engineering with the University of Liverpool, Liverpool. He was a Professor with the Department of Electrical Engineering, Tsinghua University, where he was an Assistant President and the Deputy Director with the Laboratory of Low-Carbon Energy in 2009. From 2012 to 2017, he was the Executive Vice-President of Zhejiang University, China. His current research interests include smart grid, electricity economics, and operation and control of power systems.

Prof. Song was a recipient of the D.Sc. Award from Brunel University in 2002 for his original achievements in power systems research. He was elected Vice-President of the Chinese Society for Electrical Engineering (CSEE) and appointed Chairman of the International Affairs Committee of the CSEE in 2009. In 2004, he was elected as a Fellow of the Royal Academy of Engineering, U.K.